

Synthesis and Characterization of Starch/Na-MMT Nanocomposites

Álvaro García-Padilla¹, Kariana Moreno-Sader¹, María Acevedo-Morantes¹,
Álvaro Realpe-Jimenez¹ and João B.P. Soares²

¹ Department of Chemical Engineering, Research Group of Modeling of Particles
and Processes, University of Cartagena, Cartagena, Colombia

² Group of Applied Macromolecular Engineering
Department of Chemical and Materials Engineering
University of Alberta, Donadeo Innovation Centre for Engineering
9211 - 116 St, Edmonton, Alberta, Canada

Copyright © 2018 Álvaro García-Padilla et al. This article is distributed under the Creative Commons Attribution License, which permits unrestricted use, distribution, and reproduction in any medium, provided the original work is properly cited.

Abstract

Nowadays, nanocomposites have attracted great attention to many applications as packaging material, flocculating agents and adsorbents due to its improved mechanical properties, selective adsorption, environmental friendly and low cost. The objective of this article is to synthesize a nanocomposite based on starch and sodium montmorillonite (Starch/Na-MMT) by solution intercalation technique with different biopolymer to nanoclay ratios (5:1, 10:1 and 10:3, w/w). The resulting nanomaterial was characterized by XRD, SEM, and FTIR analysis in order to observe intercalation of starch into nanoclay, morphological structure and interaction of MMT with the starch matrix, respectively. The interaction of MMT into starch matrix was confirmed by FTIR due to the presence of alumina silicate bonds in starch/Na-MMT spectrum such as Si-O, Al-Al-OH, and Si-O-Al bending. The XRD patterns indicated an exfoliation process for starch/Na-MMT (10:1 and 5:1 w/w) nanocomposites and an increase in interlayer spacing for starch/Na-MMT (10:3 w/w) nanocomposite. SEM analysis revealed a round shape and agglomerated flakes for Starch/Na-MMT.

Keywords: Nanocomposite, starch, nanoclay, sodium montmorillonite

1. Introduction

Clay minerals have been used in several types of applications such as nanocomposites [1], catalysts [2], cosmetics, paints, adsorbents for removal of hazardous compounds [3] and solving many engineering challenges in petroleum cracking [4], dehumidification and water purification [5, 6]. The high demand for clays in wide range scientific and technological areas lies in their low cost and natural abundance, high adsorption and absorption capacities, fire retardancy among other properties [7]. In the other hand, starch has been studied for the production of biodegradable products because of their low cost, being natural and a renewable carbohydrate that can be obtained from different crops such as corn, wheat, rice and bean [8]. This biopolymer could replace synthetic film of polyethylene used in packaging and in the manufacture of medical delivery systems and devices [9, 10]. Recent researches have been focused on modification of nanoclays with polymers with the aim of improving mechanical, thermal, barrier and physicochemical properties [11–12]. In this work, a nanocomposite based on starch from bean seeds and nanoclay was synthesized by solution intercalation technique and characterized by FT-IR, SEM and XRD analysis in order to obtain a low-cost nanomaterial suitable for further applications.

2. Materials and Methods

2.1. Extraction of starch

The starch from bean seeds (*Phaseolus vulgaris*) was obtained according to the methodology described by Cobana & Antezana [13]. Bean seeds were collected from a local market and soaked during 12 hours. Afterward, seed coats were removed and the seeds were milled and dried in an oven at 80°C during 24 hours. Dried starch was ground and sieved to obtain particle size less than 0.105 mm.

2.2. Synthesis of Starch/Na-MMT nanocomposite

Starch (0.5 g) was dissolved in 50 mL, 5 % vol. acetic acid (Sigma Aldrich) to form a sol by stirring at 60°C during 3 hours according to Wang et al. [14]. Then, MMT nanoclay (Southern Clays) was mixed into the sol during 24 hours to obtain different mass ratio nanocomposites (5:1, 10:1 and 10:3). The resulting mixture was dried in a vacuum oven at 70°C, ground and sieved.

2.3. Characterization techniques

FTIR analysis: The FTIR of starch, Cloisite Na⁺ and nanocomposites (5:1, 10:1 and 10:3, w/w) samples were recorded on a Cary FTIR Model 660 of Agilent technologies on attenuated total reflected (ATR) mode with 4 cm⁻¹ resolution in 4000-400 cm⁻¹ region.

XRD analysis: This technique was carried out on a Rigaku Ultima IV diffractometer with Co K α ($\lambda=0.1789$ nm) radiation in the range of 5-40° (2 Θ) angles. The d-spacing of MMT layers was determined by Bragg equation, where θ

is the diffraction angle, n is the order of diffraction and λ is the incident wavelength.

$$2d \sin(\theta) = n\lambda \quad (1)$$

SEM analysis: SEM analysis was performed on a Sigma HD Zeuss Scanning Electron Microscope at an acceleration voltage of 20 kV.

3. Results and Discussion

3.1. FT-IR analysis: Figure 1 shows the FTIR spectrum of starch, nanoclay and starch/Na-MMT nanocomposites (10:1, 5:1 and 10:3, w/w) samples.

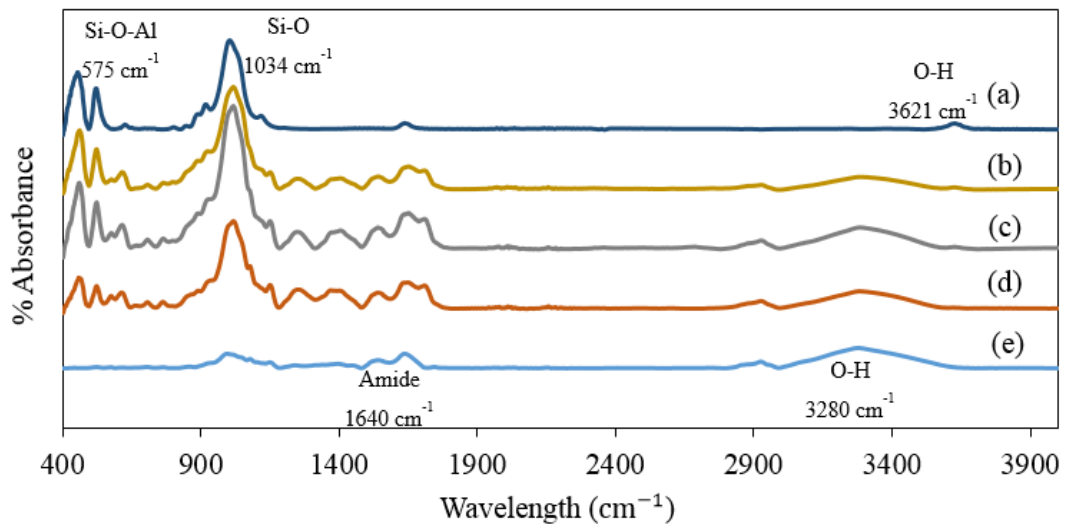


Figure 1. FTIR spectrum of (a) Na-MMT nanoclay, (b) Starch/Na-MMT (10: 3) nanocomposite, (c) Starch/Na-MMT (5: 1) nanocomposite, (d) Starch/Na-MMT (10: 1) nanocomposite and (e) Starch biopolymer.

Figure 1 (a) shows a peak at 3621 cm^{-1} attributed to O-H stretch vibration due to the high amount of Al in the octahedral layer [15, 16]. The nanocomposite samples exhibited a reduction in the intensity of this peak indicating the effects of starch addition to nanoclay by hydrogen bonds formation [17]. It has been reported bands in starch spectra in the range $3000\text{-}3600 \text{ cm}^{-1}$, which are assigned to complex stretching vibration associated with free inter and inter-molecular bound hydroxyl groups [18]. The starch spectra obtained in this work has a peak at 3280 cm^{-1} as shown Figure 1 (e) that corresponds to OH stretching vibrations of hydroxyl groups widely present in amylose and amylopectin chemical structure, which are the main constituent of starch biopolymer [19]. In addition, O-H bending of water molecules was observed at 1635 cm^{-1} for starch/Na-MMT nanocomposites [20]. According to Huang et al.[21], hydroxyl groups of starch can interact with hydroxyl groups on the surface of the clay. As is shown in Figures 1 (b-d), the C-O, C-C, C-O-H stretching

and C-O-H bending are observed around 1100-1200 cm^{-1} [22–23]. The peak at 1640 cm^{-1} is assigned to the amine group. The presence of carbonyl, alcohol and amine functional group contributes to the formation of strong hydrogen bonds and interaction with other substrates [24]. The absorbance bands at 1034, 950 and 519 cm^{-1} in nanoclay spectra is associated to Si-O stretching vibrations of the tetrahedral layer, Al-Al-OH bending and Si-O-Al bending [25–26], which also appear in nanocomposites spectra suggesting a successful synthesis due to the incorporation of polymer matrix onto Na- MMT layers [27].

3.2. XRD analysis: The XRD patterns for nanoclay, starch and nanocomposites samples are shown in Figure 2.

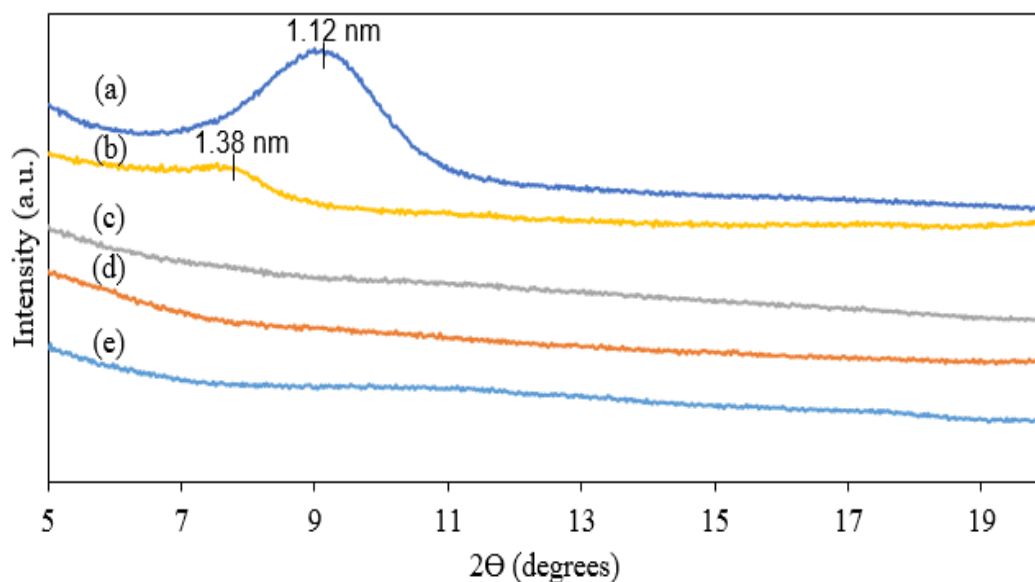


Figure 2. XRD patterns of (a) Na-MMT nanoclay, (b) Starch/Na-MMT (10:3) nanocomposite, (c) Starch/Na-MMT (5:1) nanocomposite, (d) Starch/Na-MMT (10:1) nanocomposite and (e) Starch biopolymer.

These patterns show structural variation by intercalation or exfoliation of nanoclay due to the presence of biopolymer in gallery spacing. In addition, provide information about spacing between silicate layers [27]. Figure 2 (a) exhibited an intensive peak at 2θ angle of 9.12° , which represented an interlayer spacing (d_{001}) of 1.12 nm calculated by Equation 1 [16]. The absence of this peak in starch/Na-MMT (5:1 and 10:1, w/w) indicated that the starch intercalated, exfoliated and adsorbed on the Na-MMT galleries to change the performance of clay galleries [28]. The starch/Na-MMT nanocomposite (10:3 w/w) pattern showed a shifted peak at $2\theta=7.54^\circ$, hence, an increase in interlayer spacing (1.38 nm) suggesting that starch only intercalated on Na-MMT layers remaining a laminated structure [29]. Dennis et al. [28] state that intercalation refers to the case where a small amount of polymer moves into the gallery spacing between clay platelets (less than 20-30 Å) without delamination.

3.3. SEM analysis: The SEM micrographs used to study morphology of nanocomposites are shown in Figure 3, results similar to those reported by Klein et al. [30], the bean starch exhibited a round shape with a truncated end on one side and a smooth surface with no evidence of any fissures or pores as shown in Fig 3 (a). The MMT is composed of flakes or agglomerated flakes with varied sizes. For the Starch/Na-MMT nanocomposites (10:1 and 5:1, w/w), the clay platelets are poorly dispersed and form aggregates that break upon loading, as was observed in the fracture surface of the starch composites. These results confirm the morphological change suffered by base components (nanoclay and starch) after the synthesis process.

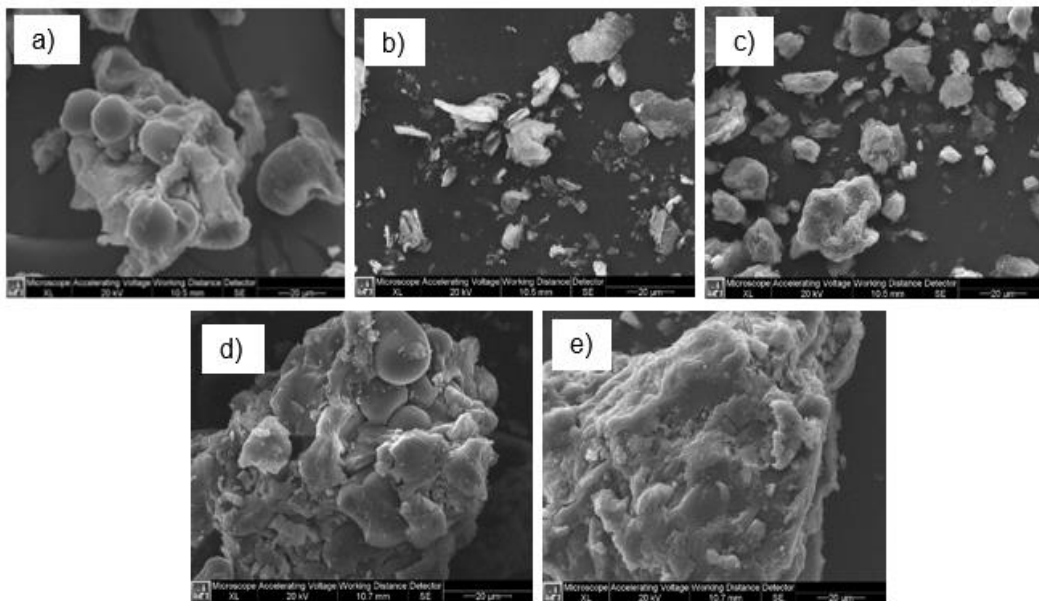


Figure 3. SEM micrographs of (a) Starch biopolymer, (b) Nanoclay (c) Starch/Na-MMT (10: 3), (d) Starch/Na-MMT (5: 1) and (e) Starch/Na- MMT (10: 1).

4. Conclusions

This work was focused on synthesizing and characterization of nanocomposites based on starch and nanoclay with many applications in packaging and wastewater treatments. The FT-IR spectrums indicated the presence of Si-O stretching vibrations of the tetrahedral layer, Al-Al-OH bending and Si-O-Al bending in nanoclay and nanocomposites (10:1, 5:1 and 10:3, w/w) samples suggesting the incorporation of polymer matrix onto Na- MMT layers. The XRD analysis was used to observe the intercalation of starch onto nanoclay. The absence of a peak at 9.12° in Starch/Na-MMT (10:1 and 5:1, w/w) patterns suggested an exfoliation process which can be attributed to the weakness of Van der Waals force. The SEM micrograph of starch revealed a round shape that is converted to aggregated flakes

when nanoclay was added during the synthesis. These results indicated a successful synthesis of nanocomposites based on starch and Na-MMT and provided information of its physicochemical characterization for further applications.

Acknowledgements. Authors express their gratitude to University of Cartagena and University of Alberta for providing financial support to develop this research.

References

- [1] S.S. Ray, M. Okamoto, Polymer / layered silicate nanocomposites : a review from preparation to processing, *Progress in Polymer Science*, **28** (2003), 1539–1641. <https://doi.org/10.1016/j.progpolymsci.2003.08.002>
- [2] G. Nagendrappa, Organic synthesis using clay and clay-supported catalysts, *Applied Clay Science*, **53** (2011), 106–138. <https://doi.org/10.1016/j.clay.2010.09.016>
- [3] A. Dabrowski, Adsorption--from theory to practice, *Advances in Colloid and Interface Science*, **93** (2001), 135–224.
- [4] A. Soriente, R. Arienzo, M. De Rosa, A. Spinella, A. Scettri, L. Palombi, K10 montmorillonite catalysis: CC bond formation by catalyzed conjugate addition and alkoxyalkylation of 1,3dicarbonyl compounds, *Green Chemistry*, **1** (1999), 157–162. <https://doi.org/10.1039/a902102g>
- [5] S.Q. Zhang, W. G. Hou, Adsorption behavior of Pb(II) on montmorillonite, *Colloids and Surfaces A: Physicochemical and Engineering Aspects*, **320** (2008), 92–97. <https://doi.org/10.1016/j.colsurfa.2008.01.038>
- [6] Q. Zhang, L. Zha, J. Ma, B. Liang, A Novel Route to the Preparation of Poly(N-isopropylacrylamide) Microgels by Using Inorganic Clay as a Cross-Linker, *Macromolecular Rapid Communications*, **28** (2007), 116–120. <https://doi.org/10.1002/marc.200600629>
- [7] C. Bilgiç, D. Topaloğlu Yazici, N. Karakehya, H. Çetinkaya, A. Singh, M. Chehimi, Surface and interface physicochemical aspects of intercalated organo-bentonite, *International Journal of Adhesion and Adhesives*, **50** (2014), 204–210. <https://doi.org/10.1016/j.ijadhadh.2014.01.033>
- [8] D. Le Corre, J. Bras, A. Dufresne, Starch Nanoparticles: A Review, *Biomacromolecules*, **11** (2010), 1139–1153. <https://doi.org/10.1021/bm901428y>

- [9] G-Q. Chen, M.K. Patel, Plastics Derived from Biological Sources: Present and Future: A Technical and Environmental Review, *Chemical Reviews*, **112** (2012), 2082–2099. <https://doi.org/10.1021/cr200162d>
- [10] M. Fishman, D. Coffin, R. Konstance, C.I Onwulata, Extrusion of pectin/starch blends plasticized with glycerol, *Carbohydrate Polymers*, **41** (2000), 317–325. [https://doi.org/10.1016/s0144-8617\(99\)00117-4](https://doi.org/10.1016/s0144-8617(99)00117-4)
- [11] L-F. Chen, H-W. Liang, Y. Lu, Chun-Hua Cui, Shu-Hong Yu, Synthesis of an Attapulgite Clay@Carbon Nanocomposite Adsorbent by a Hydrothermal Carbonization Process and Their Application in the Removal of Toxic Metal Ions from Water, *Langmuir*, **27** (2011), 8998–9004. <https://doi.org/10.1021/la2017165>
- [12] Vercelheze AES, Fakhouri FM, Dall’Antônia LH, A. Urbano, E. Youssef, F. Yamashita, S. Mali, Properties of baked foams based on cassava starch, sugarcane bagasse fibers and montmorillonite, *Carbohydrate Polymers*, **87** (2012), 1302–1310. <https://doi.org/10.1016/j.carbpol.2011.09.016>
- [13] M. Cobana, R. Antezana, Proceso de extracción de almidón de yuca por vía seca, *Revista Boliviana de Química*, **24** (2007), 77–83.
- [14] H. Wang, H. Tang, Z. Liu, Xin Zhang, Z. Hao, Z. Liu, Removal of cobalt(II) ion from aqueous solution by chitosan-montmorillonite, *Journal of Environmental Sciences (China)*, **26** (2014), 1879–1884. <https://doi.org/10.1016/j.jes.2014.06.021>
- [15] S. Silva, C. Braga, M. Fook, C. Raposo, L. Carvalho, E. Canedo, Application of infrared spectroscopy to analysis of chitosan/clay nanocomposites, Chapter in *Infrared Spectroscopy - Materials Science, Engineering and Technology*, T. Theophanides (ed), InTech, 2012. <https://doi.org/10.5772/35522>
- [16] M. Abdollahi, M. Rezaei, G. Farzi, A novel active bionanocomposite film incorporating rosemary essential oil and nanoclay into chitosan, *Journal of Food Engineering*, **111** (2012), 343–350. <https://doi.org/10.1016/j.jfoodeng.2012.02.012>
- [17] V.P. Cyras, L.B. Manfredi, M-T. Ton-That, A. Vázquez, Physical and mechanical properties of thermoplastic starch/montmorillonite nanocomposite films, *Carbohydrate Polymers*, **73** (2008), 55–63. <https://doi.org/10.1016/j.carbpol.2007.11.014>
- [18] J. Hong, X-A. Zeng, R. Buckow, Z. Han, Man-sheng Wang, Nanostructure, morphology and functionality of cassava starch after pulsed electric fields assisted acetylation, *Food Hydrocolloids*, **54** (2016), 139–150.

<https://doi.org/10.1016/j.foodhyd.2015.09.025>

- [19] A.J. García, K.A. Moreno, M. Acevedo-Morantes A. Realpe-Jimenez, Determination of some Physicochemical Properties from two Different Cranberry Bean, *Phaseolus Vulgaris* Species, *International Journal of Applied Engineering Research*, **11** (2016), 6767–6773.
- [20] M. Abdollahi, M. Rezaei, G. Farzi, A novel active bionanocomposite film incorporating rosemary essential oil and nanoclay into chitosan, *Journal of Food Engineering*, **111** (2012), 343–350.
<https://doi.org/10.1016/j.jfoodeng.2012.02.012>
- [21] M. Huang, J. Yu, X. Ma, Studies on the properties of Montmorillonite-reinforced thermoplastic starch composites, *Polymer*, **45** (2004), 7017–7023.
<https://doi.org/10.1016/j.polymer.2004.07.068>
- [22] B.J. Goodfellow, R.H. Wilson, A fourier transform IR study of the gelation of amylose and amylopectin, *Biopolymers*, **30** (1990), 1183–1189.
<https://doi.org/10.1002/bip.360301304>
- [23] W. Gao, H. Dong, H. Hou, Hui Zhang, Effects of clays with various hydrophilicities on properties of starch–clay nanocomposites by film blowing, *Carbohydrate Polymers*, **88** (2012), 321–328.
<https://doi.org/10.1016/j.carbpol.2011.12.011>
- [24] E. Assaad, A. Azzouz, D. Nistor, A.V. Ursu, T. Sajin, D.N. Miron, F. Monette, P. Niquette, R. Hausler, Metal removal through synergic coagulation–flocculation using an optimized chitosan-montmorillonite system, *Applied Clay Science*, **37** (2007), 258–274.
<https://doi.org/10.1016/j.clay.2007.02.007>
- [25] Y.M. Vargas-Rodríguez, V. Gómez-Vidales, E. Vázquez-Labastida, A. García-Bórquez, G. Aguilar-Sahagún, H. Murrieta-Sánchez and M. Salmón, Caracterización espectroscópica, química y morfológica y propiedades superficiales de una montmorillonita mexicana, *Revista Mexicana de Ciencias Geológicas*, **25** (2008), 135–144.
- [26] S. Tunç, O. Duman, The effect of different molecular weight of poly(ethylene glycol) on the electrokinetic and rheological properties of Na-bentonite suspensions, *Colloids and Surfaces A: Physicochemical and Engineering Aspects*, **317** (2008), 93–99. <https://doi.org/10.1016/j.colsurfa.2007.09.039>
- [27] A.M. Atta, H.A. Al-Lohedan, Z.A. ALothman, A. Abdel-Khalek, A. Tawfeek, Characterization of reactive amphiphilic montmorillonite nanogels and its application for removal of toxic cationic dye and heavy metals water

- pollutants, *Journal of Industrial and Engineering Chemistry*, **31** (2015), 374–384. <https://doi.org/10.1016/j.jiec.2015.07.012>
- [28] H.R. Dennis, D.L. Hunter, D. Chang, S. Kim, J.L. White, J.W. Cho, D.R. Paul, Effect of melt processing conditions on the extent of exfoliation in organoclay-based nanocomposites, *Polymer*, **42** (2001), 9513–9522. [https://doi.org/10.1016/s0032-3861\(01\)00473-6](https://doi.org/10.1016/s0032-3861(01)00473-6)
- [29] J.H. Park, S.C. Jana, Mechanism of exfoliation of nanoclay particles in epoxy-clay nanocomposites, *Macromolecules*, **36** (2003), 2758–2768. <https://doi.org/10.1021/ma021509c>
- [30] B. Klein, N.L. Vanier, K. Moomand, V. Pinto, R. Colussi, E. Zavareze, A. Dias, Ozone oxidation of cassava starch in aqueous solution at different pH, *Food Chemistry*, **155** (2014), 167–173. <https://doi.org/10.1016/j.foodchem.2014.01.058>

Received: March 26, 2018; Published: May 18, 2018